

N-Amination of Peptides: A Theoretical Study

Carlos Alemán*

Departament d'Enginyeria Química, E.T.S.E.I.B, Universitat Politècnica de Catalunya, Diagonal 647, Barcelona E-08028, Spain

Received: October 19, 2001

A quantum mechanical study about the effects of replacing the amide link by the *N*-amino amide group in peptides is presented. More specifically, this work deals with (i) the isomerization process of the *N*-amino amide link and (ii) the conformational changes induced by *N*-amination on both the glycine- and proline-containing dipeptides. Molecular geometries were optimized at both HF/6-31G(d) and MP2/6-31G(d) levels of theory. High-level ab initio calculations were performed on the optimized geometries in order to investigate the effects of both the basis set and electron correlation on the relative energies. Furthermore, the reliability of the density functional approximation on the conformational studies of *N*-amino peptides was investigated by considering six different functionals. Calculations in solution (dielectric constants of $\epsilon = 2, 4, 8, 33,$ and 78.5) were performed using the polarizable continuum model in the framework of the ab initio HF/6-311++G-(d,p) level.

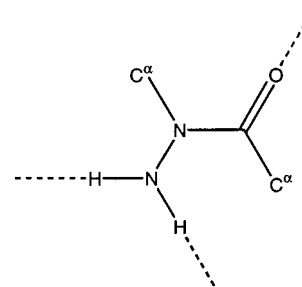
Introduction

In recent years, there has been considerable interest in the conformational properties of both naturally occurring and modified amino acids. The study of the formers has been mainly driven by a desire to understand the hydrogen-bonding properties of the constituents of peptides and proteins.¹ On the other hand, modified amino acids are of relevant interest for their use as building blocks in molecular engineering since they can be used to control the peptide secondary structure² and to design molecules with enhanced resistance to biodegradation but retaining the receptor binding ability and biological response of native peptides.³ The design of all these compounds requires the advanced knowledge of the impact on the amino acid conformations of such modifications.

Modifications may involve changes in the amino acid side chain or alteration of the peptide bond. A potential advantage of the latter is that introduction of modified peptide links makes it possible to influence the biological properties of a molecule but retaining the receptor binding ability, which usually depends of the side chains.⁴ The most common modified amide bond is the retromamide, which has been subject of a number of both experimental and theoretical studies.^{5,6} Thus, the conformational impact of retromodification on different amino acids, i.e., glycine, alanine, valine, and dehydroalanine, has been investigated using ab initio quantum mechanical calculations.⁶

Contrary to retromodification, it is surprising to see how little attention has received *N*-amination. It is worth noting that *N*-amination can induce important conformational changes because this modification of the peptide bond produces important alterations in the intra- and interhydrogen bonding networks (Scheme 1). This topic was investigated by introducing *N*-amino amide links into simple peptides and analyzing the induced conformational perturbations in both solution and solid state.⁷ Results allowed to conclude that the *N*-amino amide link has a potential interest in the design of peptidomimetics when the side chains are required for bioactivity and cannot be modified.

SCHEME 1: Hydrogen Bonding Scheme for the *N*-Amino Amide Group



However, it should be mentioned that *N*-amino peptides are not easily obtained when the α -carbon bears a side chain. Thus, from a synthetic point of view, the *N*-amino group must be introduced before *N*-coupling, the yield of *N*-amino peptide being particularly small due to the low accessibility and nucleophilicity of the NH group connected to the α -carbon.

In this work, I wish to provide a complete theoretical study about the *N*-amination. First, the energetics and structural changes associated to the isomerization process of the *N*-amino amide link have been investigated by considering the *N*-amino peptide derived from *N*-methylacetamide (**1**). Results have been compared with those obtained for the amide link. Next, a study about the conformational changes induced by *N*-amination in simple peptides has been undertaken. For this purpose, an extensive quantum mechanical investigation on the *N*-amino glycine-containing dipeptide (**2**) has been performed using both ab initio and DFT methods. This compound was chosen because the conformational properties of unmodified glycine-containing dipeptide (**3**) are well-known. Thus, it is the dipeptide most studied by high-level ab initio calculations.⁸ Finally, to investigate the dependence between the conformational changes induced by *N*-amination and the position of the *N*-amino amide group in the chain, two additional peptides have been considered. These are the proline-containing dipeptide (**4**) and the analogue with the *N*-amino amide link at the C-terminal position (**5**).

* Corresponding author. E-mail: aleman@eq.upc.es.

Results have been compared with those previously reported by X-ray crystallography.^{7a,9}

Methods

Calculations were performed on an IBM/SP2 and a HP-V2500 computer of the Centre de Supercomputació de Catalunya (CESCA) using the Gaussian 98 program.¹⁰ Molecular geometries of all the conformations considered for **1** and **2** were optimized in the gas phase at both the HF/6-31G(d)¹¹ and MP2/6-31G(d)¹² levels of theory, while conformations of **4** and **5** were only optimized at the former level. The default force and displacement termination criteria within Gaussian 98 were used for all optimizations. All the stationary points located at the HF/6-31G(d) level were characterized as minima or transition states by harmonic vibrational frequency calculations. Frequency analysis was also used to provide the zero-point vibrational energy (ZPE), the thermal correction to the energy, and the entropy following the standard formulas (the imaginary frequency at the transition states was removed from the frequency analysis). Single-point energy calculations were performed on the MP2/6-31G(d) geometries at the HF/6-311G(d,p), MP2/6-311G(d,p), HF/6-311++G(d,p), MP2/6-311++G(d,p), and MP4/6-31G(d) levels of theory. Thus, the best estimate to the energy was that with the MP2 corrections computed from the 6-311++G(d,p) basis set and the small correction up to MP4 calculated at the 6-31G(d) level and added to the MP2/6-311++G(d) energy. The final value is denoted as MP2/6-311++G(d,p)+MP4#//MP2/6-31G(d).

The relative energies for minimum-energy conformations of **2** have been investigated using density functional theory (DFT). In this study, we have used the following combinations: Slater–Dirac (S) exchange¹³ and Vosko, Wilk, and Nusair (VWN) correlation functional¹⁴ (S–VWN); Becke (B) exchange¹⁵ and VWN correlation functional (B–VWN); Becke’s three-parameter hybrid functional with gradient corrections provided by the Lee, Yang, and Parr (LYP) functional¹⁶ (B3-LYP);¹⁷ S exchange and LYP gradient correction to correlation (S-LYP); B exchange and Perdew and Wang’s (PW91) gradient correction to correlation¹⁸ (B-PW91); and S exchange and PW91 correlation (S-PW91). DFT calculations were performed with both the 6-31G(d) and 6-311++G(d,p) basis sets and using the molecular geometries optimized at the MP2/6-31G(d) level.

The effect of the solvent in conformational preferences of the compounds under study was estimated following the polarizable continuum model (PCM) developed by Tomasi and co-workers.¹⁹ PCM calculations were performed in the framework of the ab initio HF level with the 6-311++G(d,p) basis set. Calculations were performed with the following dielectric constants: $\epsilon = 2$ for CCl₄, $\epsilon = 4$ for CHCl₃, $\epsilon = 8$ for CH₂Cl₂, $\epsilon = 33$ for CH₃OH and $\epsilon = 78.5$ for H₂O.

Results and Discussion

N-Amino Amide Bond Isomerization. An interesting characteristic of the *N*-amino amide bond is that it is able to adopt two trans conformations, which are displayed in Figure 1. As can be seen, in these arrangements the lone pair (trans₁) or the hydrogen atoms (trans₂) of the *N*-amino moiety are closest to the carbonyl carbon atom. Accordingly, eight conformations were considered for **1**: four minima (trans₁, trans₂, cis₁ and cis₂) and four transition states (TS_{anti,1}, TS_{anti,2}, TS_{syn,1} and TS_{syn,2}). The MP2/6-31G(d) optimized geometries are displayed in Figure 1, the main geometrical parameters being listed in Table 1. The values of the C^α–C–N–C^α dihedral angle, denoted ω_1 in Scheme 2, and C–N–C^α bond angle at the transition states are

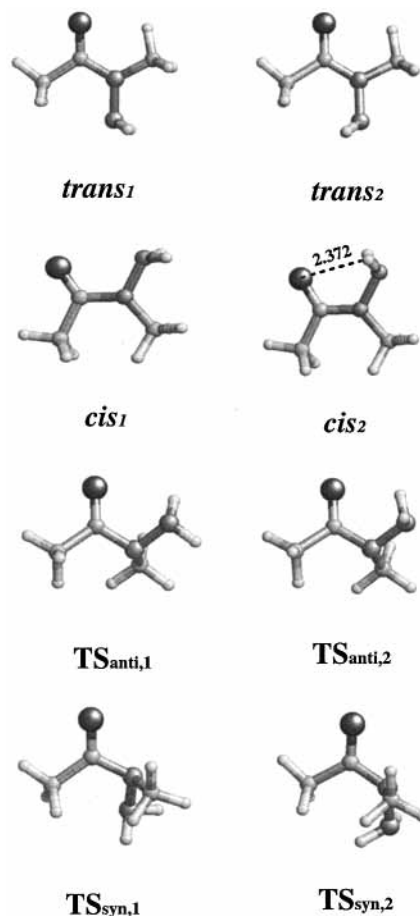
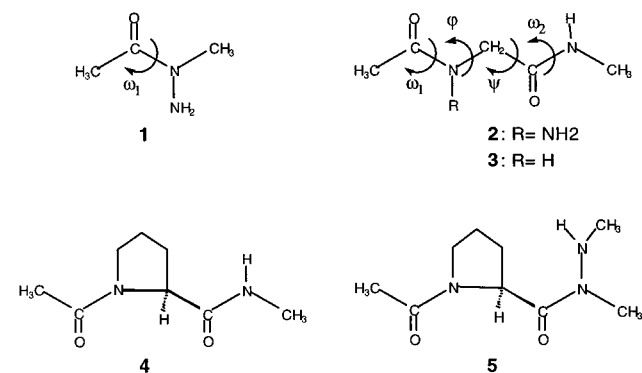


Figure 1. MP2/6-31G(d) optimized minima and transition states of **1**. Distance in Å.

SCHEME 2: Compounds under Study



consistent with the change from sp² to sp³ hybridization. Furthermore, the C–N bond length elongates around 0.07 Å when the conjugation is broken.

Enthalpy differences are listed in Table 2. In all cases, the trans₁ conformation is more stable than the trans₂, the enthalpy difference being 1.4 kcal/mol at the MP2/6-311++G(d,p)+MP4#//MP2/6-31G(d) level. This enthalpy difference is overestimated by 0.8 kcal/mol at the HF level independently of both the basis set used in energy calculations and the level of geometry optimization. The cis₁ conformation is 6.0 kcal/mol less stable than the trans₁ at the best level of theory. The low stability of this structure is mainly due to the repulsive interactions between the electron lone pairs of the *N*-amino group and the oxygen atom. The fourth energy minimum is the cis₂, which is clearly stabilized by an electrostatic interaction of C₅ type (five-membered hydrogen bonded ring) between one

TABLE 1: Geometrical Parameters of the Eight Stationary Points of 1 Resulting from MP2/6-31G(d) Optimizations^a

parameter	trans ₁	trans ₂	TS _{anti,1}	TS _{anti,2}	TS _{syn,1}	TS _{syn,2}	cis ₁	cis ₂
$d(\text{C}^\alpha\text{-C})$	1.512	1.518	1.506	1.506	1.512	1.519	1.519	1.514
$d(\text{C=O})$	1.233	1.234	1.222	1.226	1.221	1.222	1.226	1.236
$d(\text{C-N})$	1.378	1.374	1.437	1.437	1.440	1.439	1.392	1.375
$d(\text{N-N})$	1.406	1.410	1.436	1.443	1.465	1.433	1.411	1.421
$d(\text{N-C}^\alpha)$	1.449	1.452	1.474	1.474	1.437	1.465	1.455	1.453
$\angle\text{C}^\alpha\text{-C-N}$	116.2	116.0	113.5	113.8	117.8	118.6	115.6	117.1
$\angle\text{O-C-N}$	122.7	122.1	122.3	122.4	118.9	119.3	115.6	117.1
$\angle\text{C-N-C}^\alpha$	121.4	121.4	109.7	110.8	111.2	111.1	123.3	125.2
$\angle\text{C-N-N}$	119.3	124.1	108.2	111.9	109.9	115.4	115.4	117.3
$\angle\text{C}^\alpha\text{-C-N-C}^\alpha$	180.0	180.0	90.0	90.0	-90.0	-90.0	22.9	18.1

^a Bond lengths are in Å, and bond angles and torsional angles are in deg.

TABLE 2: Enthalpy Differences^a (in kcal/mol) in the Gas Phase among the Eight Conformations of 1 Computed from Different Theoretical Levels^a

level	trans ₁	trans ₂	TS _{anti,1}	TS _{anti,2}	TS _{syn,1}	TS _{syn,2}	cis ₁	cis ₂
HF/6-31G(d)//HF/6-31G(d) ^b	0.0	2.2	14.3	11.4	15.8	18.2	8.0	0.9
	$\omega_1 = 180^\circ$	$\omega_1 = 180^\circ$	$\omega_1 = 90^\circ$	$\omega_1 = 90^\circ$	$\omega_1 = -90^\circ$	$\omega_1 = -90^\circ$	$\omega_1 = 13.6^\circ$	$\omega_1 = 12.0^\circ$
MP2/6-31G(d)//HF/6-31G(d) ^c	0.0	1.8	14.1	10.6	15.6	17.9	7.7	0.3
MP2/6-31G(d)//MP2/6-31G(d) ^d	0.0	1.7	13.5	10.0	15.2	17.4	7.5	0.1
	$\omega_1 = -180^\circ$	$\omega_1 = 180^\circ$	$\omega_1 = 90^\circ$	$\omega_1 = 90^\circ$	$\omega_1 = -90^\circ$	$\omega_1 = -90^\circ$	$\omega_1 = 22.9^\circ$	$\omega_1 = 18.1^\circ$
HF/6-311G(d,p)//MP2/6-31G(d) ^e	0.0	2.2	16.1	12.0	18.3	18.1	7.9	1.5
MP2/6-311G(d,p)//MP2/6-31G(d) ^f	0.0	1.5	12.6	9.8	16.3	14.5	6.9	0.4
HF/6-311++G(d,p)//MP2/6-31G(d) ^g	0.0	2.2	14.3	12.0	15.9	18.1	7.7	1.2
MP2/6-311++G(d,p)//MP2/6-31G(d) ^h	0.0	1.4	11.9	9.6	13.8	15.7	6.2	-0.2
MP4/6-31G(d)//MP2/6-31G(d) ⁱ	0.0	1.6	12.8	9.4	14.6	16.7	7.3	0.0
MP2/6-311++G(d,p)+MP4#//MP2/6-31G(d) ^j	0.0	1.4	11.3	8.9	13.2	15.1	6.0	-0.3

^a Zero-point energies and thermal corrections at 298 K computed at the HF/6-31G(d) level are included. All the values are relative to the trans₁ conformation. The values of the dihedral angle ω_1 (in deg) resulting from HF/6-31G(d) and MP2/6-31G(d) geometry optimizations are displayed in parenthesis. ^b $E = -301.898400$ au. ^c $E = -302.783190$ au. ^d $E = -302.786406$ au. ^e $E = -301.977824$ au. ^f $E = -302.972199$ au. ^g $E = -301.984267$ au. ^h $E = -302.986172$ au. ⁱ $E = -302.864747$ au. ^j $E = -303.064513$ au.

TABLE 3: Free Energy Differences (in kcal/mol) at 298 K in the Gas Phase and Aqueous Solution among the Eight Conformations of 1^a

#	trans ₁	trans ₂	TS _{anti,1}	TS _{anti,2}	TS _{syn,1}	TS _{syn,2}	cis ₁	cis ₂
ΔH_{gp}^b	0.0	1.4	11.9	8.9	13.2	14.1	6.0	-0.3
$-T\Delta S_{\text{gp}}(T = 298\text{ K})^c$	0.0	-0.5	1.6	1.5	1.6	1.7	0.1	0.0
ΔG_{gp}^d	0.0	0.8	13.5	10.6	14.8	16.8	6.1	-0.3
$\Delta G_{\text{sol,aq}}^e$	-10.2	-10.8	-10.3	-8.2	-10.3	-11.3	-14.3	-9.6
$\Delta\Delta G_{\text{sol,aq}}$	0.0	-0.7	-0.1	1.9	-0.2	-1.1	-4.1	0.5
ΔG_{aq}^f	0.0	0.2	13.4	12.6	14.6	15.7	2.0	0.2

^a Enthalpy and entropic correction differences in the gas phase and free energies of solvation in aqueous solution are also displayed (in kcal/mol). All the values are relative to the trans₁ conformation. ^b Enthalpies at 298 K in the gas phase calculated at the MP2/6-31++G(d,p)+MP4#//MP2/6-31G(d) level (see Table 1). ^c Entropic corrections at 298 K calculated at the HF/6-31G(d)//HF/6-31G(d) level. ^d Free energy differences at 298 K in the gas phase: $\Delta G_{\text{gp}} = \Delta H_{\text{gp}} - T\Delta S_{\text{gp}}$. ^e Free energies of solvation in aqueous solution computed from the PCM model at the HF/6-311++G(d,p) level. ^f Free energy difference at 298 K in aqueous solution: $\Delta G_{\text{aq}} = \Delta G_{\text{gp}} + \Delta\Delta G_{\text{sol,aq}}$.

of the hydrogen atoms belonging to the *N*-amino moiety and the oxygen atom of the carbonyl group (Figure 1). As a result, this is the most stable conformation at the MP2/6-311++G(d,p)+MP4#//MP2/6-31G(d) level, the enthalpy difference with respect to the trans₁ being -0.3 kcal/mol. It is worth noting that the enthalpy of the two cis conformations strongly depends on the level of theory. Thus, the omission of electron correlation effects and the use of a small basis set induce a destabilization of about 2 kcal/mol.

The enthalpy differences of the transition states TS_{anti,1}, TS_{anti,2}, TS_{syn,1}, and TS_{syn,2} with respect to the trans₁ minimum are 11.3, 8.9, 13.2, and 15.1 kcal/mol at the best level of theory. Accordingly, the TS_{anti,1} and TS_{anti,2} are the most favored route for the cis₁ ↔ trans₁ and cis₂ ↔ trans₂ interconversions, respectively. Comparison between the results obtained at the MP2/6-311++G(d,p)+MP4#//MP2/6-31G(d) and HF/6-311++G(d,p)//MP2/6-31G(d) levels indicates that electron correlation reduces the enthalpy differences of the transition states by about 3 kcal/mol. On the other hand, results displayed in Table 2

reveals that the use of a small basis set can induce an overestimation of about 1.5 kcal/mol.

Table 3 shows the entropic contribution in the gas phase, $-T\Delta S_{\text{gp}}$, at 298 K for the eight stationary points of 1. This correction notably increases the rotational barriers (around 1.5–1.7 kcal/mol at 298 K). The free energies for the isomerization of the *N*-amine amide bond in the gas phase, ΔG_{gp} , are included in Table 3. These values have been obtained by combining the enthalpy differences derived from MP2/6-311++G(d,p)+MP4#//MP2/6-31G(d) calculations and the entropic contributions provided by HF/6-31G(d)//HF/6-31G(d) frequency calculations.

Results indicate the enthalpic nature of the isomerization of the *N*-amino amide bond. The cis₂ is the most stable minimum, being favored with respect to the trans₁, trans₂ and cis₁ structures by 0.3, 1.1, and 6.4 kcal/mol, respectively. On the other hand, the TS_{anti,2} is the most stable transition state by 2.9–6.2 kcal/mol. Atomic charges and dipole moments revealed that the preferences for the TS_{anti,2} in the gas phase may be explained by the larger charge separation in the other transition states.

Thus, the dipole moments of the TS_{anti,1}, TS_{anti,2}, TS_{syn,1}, and TS_{syn,2} transition states are 3.85, 2.28, 4.70, and 4.00 D, respectively. The free energy barriers for the cis₁-to-trans₁ and cis₂-to-trans₂ interconversions are 7.4 and 10.9 kcal/mol, respectively, while barriers for the trans₁-to-cis₁ and trans₂-to-cis₂ isomerisms are 13.5 and 9.8 kcal/mol, respectively.

The free energies of solvation in aqueous solution ($\Delta G_{\text{sol,aq}}$) from PCM/6-311++G(d,p) calculations for the eight stationary points are listed in Table 3. The trans₂ and cis₁ conformers are stabilized relative to the trans₁ by 0.6 and 4.1 kcal/mol, whereas the cis₂ minimum is destabilized by 0.6 kcal/mol. These $\Delta G_{\text{sol,aq}}$ differences are not fully consistent with the relative variation of the molecular dipoles predicted at the HF/6-311++G(d,p): 4.56 (trans₁), 4.02 (trans₂), 5.65 (cis₁), and 3.31 (cis₂) D. Thus, $\Delta G_{\text{sol,aq}}$ values are also influenced by the accessibility of the polar atoms involved in the *N*-amino amide bond to the bulk water.

The free energy differences in aqueous solution (ΔG_{aq}), which were estimated with the classical thermodynamical scheme by adding the $\Delta \Delta G_{\text{sol,aq}}$ to the corresponding ΔG_{gp} , are included in Table 3. Results indicate that the trans₂ and cis₂ conformations are only 0.2 kcal/mol less stable than the trans₁ one, which is the lowest-energy minimum. On the other hand, the free energy difference of the cis₁ conformation decreases from 6.1 kcal/mol in the gas phase to 2.0 kcal/mol in aqueous solution.

The $\Delta G_{\text{sol,aq}}$ values predicted for the four transition states are also explained by the accessibility of the polar atoms to the bulk solvent rather than by the dipole moments (3.85, 2.28, 4.70, and 4.00 D for the TS_{anti,1}, TS_{anti,2}, TS_{syn,1}, and TS_{syn,2}, respectively). Results in Table 3 show that the TS_{anti,2} is destabilized with respect to the trans₁ by 2.0 kcal/mol whereas the stability of TS_{syn,2} is increased by 1.1 kcal/mol. On the other hand, the stability of TS_{anti,1} and TS_{syn,1} in aqueous solution remains practically unaltered with respect to the gas phase. Thus, ΔG_{aq} values indicate that the preferred routes for the cis₁ ↔ trans₁ and cis₂ ↔ trans₂ interconversions in aqueous solution are the TS_{anti,1} and TS_{anti,2}, respectively. The trans₁-to-cis₁ and the trans₂-to-cis₂ conversions have free energy barriers in water of 13.4 and 12.6 kcal, respectively, whereas the cis₁-to-trans₁ and the cis₂-to-trans₂ barriers have 11.4 and 12.4 kcal/mol, respectively.

The isomerization of the amide group was examined by a number of experimental and theoretical works.²⁰ Resonance Raman spectroscopic studies²⁰ⁱ indicated that the free energy difference in aqueous solution between the cis and trans conformation is 2.6 ± 0.4 and 3.1 ± 0.5 kcal/mol for *N*-methylacetamide and glycylglycine, respectively, in good agreement with previous theoretical determinations.^{20c,20f} These energy gaps are similar to that predicted between the cis₁ and trans₁ conformations of **1** (2.0 kcal/mol) but larger than that obtained for the cis₂ and trans₂ conformations (<0.05 kcal/mol). A common trend between the rotational isomerisms of the *N*-amino amide and the amide bonds is that the TS_{anti} is the most favored route for the cis ↔ trans interconversion in both gas phase and aqueous solution.²⁰ However, the energy barriers of the amide and the *N*-amino amide bonds are closer in aqueous solution than in the gas phase. Thus, the free energy barrier predicted in the gas phase^{20f} for the trans-to-cis interconversion of the amide bond is 17.7 kcal/mol, while for the cis-to-trans isomerism is 15.2 kcal/mol. These values, which are in good agreement with those provided by NMR studies in 1,2-dichloroethane,^{20a} are several kcal/mol larger than those obtained for the isomerization of **1**. On the other hand, activation barriers of 13.8 ± 0.8 and 11.0 ± 0.7 kcal/mol were measured for

TABLE 4: Torsional Angles^a and Relative Enthalpies^b for the Minimum-Energy Conformations of the Dipeptide Model **2 Obtained at the HF/6-31G(d) and MP2/6-31G(d) Levels**

# ^c	ω_1	φ	ψ	ω_2	ΔE^d
HF/6-31G(d)/HF/6-31G(d)					
t_1/γ_L	176.6	-85.5	95.0	-172.4	0.0 ^e
c_2/ϵ_D	20.6	79.6	155.1	-178.9	2.8
t_2/ϵ_D	-166.6	76.4	-172.7	176.7	3.0
c_2/α_L	-9.1	-86.7	-65.4	175.6	3.2
t_2/γ_D	177.4	88.3	-52.9	-173.9	4.5
t_2/α_D	176.3	111.0	35.3	173.0	7.4
MP2/6-31G(d)/MP2/6-31G(d)					
t_1/γ_L	172.6	-80.7	93.8	-170.0	0.0 ^f
c_2/ϵ_D	28.1	73.6	155.0	-178.7	3.6
t_2/ϵ_D	-164.2	68.4	-168.1	176.7	4.4
c_2/α_L	-24.2	-68.8	-56.6	175.4	2.3
t_2/γ_D	178.4	85.3	-57.1	-176.0	5.0
t_2/α_D	175.8	117.5	39.7	173.9	8.1

^a In units of deg. ^b In units of kcal/mol. ^c The structures have been labeled as ω_1 conformation/ φ, ψ conformation (see text). ^d Zer-point energies and thermal corrections computed at the HF/6-31G(d) level are included. ^e $E = -508.612890$ au. ^f $E = -510.094705$ au.

aqueous solutions of *N*-methylamide and glycylglycine, respectively, by using UV resonance Raman,²⁰ⁱ these values being similar to those obtained for **1** (13.4 and 12.4 kcal/mol).

Conformational Changes Induced by *N*-Amination in Glycine. A systematic exploration of the conformational space was performed in order to characterize the minimum-energy conformations of **2**. Because each of the two flexible dihedral angles φ and ψ is expected to have three minima, $3 \times 3 = 9$ minima can be anticipated for the potential energy hypersurface (PEHS) $E = E(\varphi, \psi)$. However, the results of the previous section showed that the dihedral angle ω_1 , which is associated to the *N*-amino amide bond, is able to adopt four minimum-energy conformations, the three more stable being very close in energy, i.e., trans₁, trans₂, and cis₂. The latter three minima have been considered in the conformational analysis of **2**, the $3 \times 3 \times 3 = 27$ structures resulting for the PEHS $E = E(\omega_1, \varphi, \psi)$ being taken as starting points in geometry optimizations.

Geometry optimizations at the HF/6-31G(d) level provided six minima, whose dihedral angles are displayed in Table 4. These structures were labeled according to the conformations associated to the dihedral angles ω_1 , φ , and ψ . The conformations of the *N*-amino amide group (ω_1) were classified using the trans₁ (t_1), trans₂ (t_2), cis₁ (c_1) and cis₂ (c_2) description. The conformation associated to the flexible dihedral angles φ and ψ were denoted according to the convention proposed by Csizmadia²³ and co-workers rather than by the nomenclature usually employed for dipeptides constituted by nonmodified amino acids,^{8,24} i.e., C₅, C₇, P_{II}, and α . This is because some of the conformations obtained for **2** are considerably different from those usually observed for such dipeptides. Accordingly, the convention used for the angles φ, ψ was as follows: $\alpha_D \approx 60^\circ, 60^\circ$; $\epsilon_D \approx 60^\circ, 180^\circ$; $\gamma_D \approx 60^\circ, -60^\circ$; $\delta_D \approx 180^\circ, -60^\circ$; $\beta_L \approx 180^\circ, 180^\circ$; $\delta_L \approx 180^\circ, 60^\circ$; $\alpha_L \approx -60^\circ, -60^\circ$; $\epsilon_L \approx -60^\circ, 180^\circ$; and $\gamma_D \approx -60^\circ, 60^\circ$.

The six HF/6-31G(d) structures were used as starting points for full optimization at the MP2/6-31G(d) level. The dihedral angles of the six MP2/6-31G(d) minima are included in Table 4. As can be seen, the MP2/6-31G(d) results are close to the HF/6-31G(d) ones. Thus, the mean change in the dihedral angles is less than 5.8°, and the largest change, which corresponds to the c_2/α_L minimum, is 17.9°. Relative enthalpies estimated from single-point calculations at different ab initio levels are shown in Table 5.

TABLE 5: Relative Enthalpies^a (in kcal/mol) in the Gas Phase for the Six Minimum-Energy Conformations of the Dipeptide Model 2

level	t_1/γ_L	c_2/ϵ_D	t_2/ϵ_D	c_2/α_L	t_2/γ_D	t_2/α_D
HF/6-31G(d)//HF/6-31G(d) ^b	0.0	2.8	3.0	3.2	4.5	7.4
MP2/6-31G(d)//HF/6-31G(d) ^c	0.0	3.5	4.2	2.9	4.8	8.0
HF/6-31G(d)//MP2/6-31G(d) ^d	0.0	2.7	2.8	4.3	4.2	7.2
MP2/6-31G(d)//MP2/6-31G(d) ^e	0.0	3.6	4.4	2.3	5.0	8.1
HF/6-311G(d,p)//MP2/6-31G(d) ^f	0.0	2.8	2.4	4.3	4.0	7.1
MP2/6-311G(d,p)//MP2/6-31G(d) ^g	0.0	3.4	3.8	2.1	4.6	7.5
HF/6-311++G(d,p)//MP2/6-31G(d) ^h	0.0	2.4	1.9	4.0	3.4	6.5
MP2/6-311++G(d,p)//MP2/6-31G(d) ⁱ	0.0	2.6	2.9	1.9	3.8	7.2
MP4/6-31G(d)//MP2/6-31G(d) ^j	0.0	3.5	4.2	2.3	5.0	7.9
MP2/6-311++G(d,p)+MP4 [#] //MP2/6-31G(d) ^k	0.0	2.5	2.7	1.9	3.8	7.0
B3LYP/6-31G(d)//MP2/6-31G(d) ^l	0.0	4.0	4.6	2.1	4.0	6.9
B3LYP/6-311++G(d,p)//MP2/6-31G(d) ^m	0.0	3.5	3.5	1.8	2.8	5.6
SLYP/6-31G(d)//MP2/6-31G(d) ⁿ	0.0	6.1	6.4	0.7	5.1	8.3
SLYP/6-311++G(d,p)//MP2/6-31G(d) ^o	0.0	5.1	4.8	0.5	3.8	7.0
BVWN/6-31G(d)//MP2/6-31G(d) ^p	0.0	3.8	4.6	1.8	3.4	6.0
BVWN/6-311++G(d,p)//MP2/6-31G(d) ^q	0.0	3.3	3.6	1.4	2.3	4.7
SVWN/6-31G(d)//MP2/6-31G(d) ^r	0.0	5.6	6.0	0.8	4.5	7.5
SVWN/6-311++G(d,p)//MP2/6-31G(d) ^s	0.0	4.9	4.6	0.6	3.4	6.4
B3PW91/6-31G(d)//MP2/6-31G(d) ^t	0.0	3.9	4.6	1.8	3.8	6.5
B3PW91/6-311++G(d,p)//MP2/6-31G(d) ^u	0.0	3.6	3.6	1.7	2.9	5.7
SPW91/6-31G(d)//MP2/6-31G(d) ^v	0.0	5.9	6.3	0.3	4.9	7.9
SPW91/6-311++G(d,p)//MP2/6-31G(d) ^w	0.0	5.3	5.0	0.2	3.9	7.0

^a Zero-point energies and thermal corrections computed at the HF/6-31G(d) level are included. ^b $E = -508.612890$ au. ^c $E = -510.088045$. ^d $E = -508.605566$ au. ^e $E = -510.094705$ au. ^f $E = -508.740554$ au. ^g $E = -510.387270$ au. ^h $E = -508.750488$ au. ⁱ $E = -510.411356$ au. ^j $E = -510.216845$ au. ^k $E = -510.533495$ au. ^l $E = -511.651551$ au. ^m $E = -511.814708$ au. ⁿ $E = -505.037729$ au. ^o $E = -505.211887$ au. ^p $E = -515.429578$ au. ^q $E = -515.599981$ au. ^r $E = -508.982960$ au. ^s $E = -509.149460$ au. ^t $E = -511.460350$ au. ^u $E = -511.613459$ au. ^v $E = -505.166233$ au. ^w $E = -505.325089$ au.

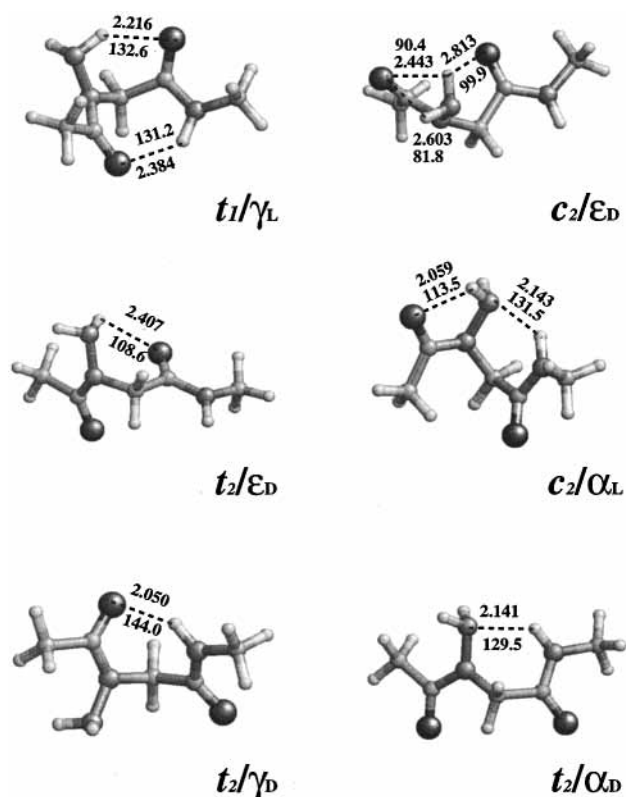


Figure 2. MP2/6-31G(d) optimized minima of the dipeptide 2. Distances and angles in Å and deg, respectively.

Figure 2 shows the six minima located for 2. The lowest-energy conformation, denoted t_1/γ_L , is stabilized by two intramolecular interactions. Thus, it forms a C_7 hydrogen bonded ring, involving the NH of the amide group and the C=O of the *N*-amino amide group, and a C_6 ring, in which the hydrogen bond is set between the *N*-amino moiety group and the C=O of the amide group. As can be seen in Figure 2, the hydrogen

bonding parameters are slightly more favorable for the latter interaction than for the former one. It is worth noting that calculations including electron correlation effects also predict the γ_L , usually denoted C_7 , as the most stable conformation for the unmodified dipeptide 3.⁸ Indeed, the dihedral angles predicted for such conformation ($\varphi, \psi = -85.5^\circ, 72.0^\circ$) are similar to those listed in Table 4 for the t_1/γ_L conformation of 2. On the other hand, in the crystal structure of the *N*-amino alanine-containing peptide (Z)-Pro- ψ [CO-N(NH₂)]-Ala-NHⁱ-Pr, the *N*-amino residue was almost extended with a C_6 ring, the latter being a consequence of the intramolecular hydrogen bond between the *N*-amino moiety group and the C=O of the amide group.²⁵ The c_2/ϵ_D conformation, which is 2.5 kcal/mol less stable than the global minimum at the best level of theory, presents three weak electrostatic interactions between the hydrogen atoms of the *N*-amino amide group and the oxygen atoms. The t_2/ϵ_D conformation can be derived from the c_2/ϵ_D one by rotating the dihedral angle associated to the *N*-amino amide group from cis_2 to $trans_2$. This change lead to the loss of two electrostatic interactions but allows a small rearrangement of the dihedral angle ψ enhancing the strength of the third one. Accordingly, the t_2/ϵ_D structure is less stable than the c_2/ϵ_D one by only 0.2 kcal/mol at the MP2/6-311++G(d,p)+MP4[#]/MP2/6-31G(d) level.

Conformation c_2/α_L , which is 1.9 kcal/mol less stable in the gas phase than t_1/γ_L , presents both C_5 and C_6 hydrogen bonding rings. The two atoms involved in the former belong to the *N*-amino amide group, whereas the latter corresponds to the interaction between the hydrogen atom of the amide group and the nitrogen lone pair of the *N*-amino moiety. Conformer t_2/γ_D is destabilized by 3.8 kcal/mol with respect to the global minimum. However, the dihedral angles of t_2/γ_D are similar to those of t_1/γ_L but of opposite sign. Furthermore, in the t_2/γ_D arrangement, the hydrogen atoms of the *N*-amino moiety are in front of the methyl end group, while in the t_1/γ_L conformation one of these atoms interacts with the amide group. Consequently, the former conformation is not able to form the C_6 hydrogen-

bonded ring and only presents a C₇ ring. The t_2/α_D conformation is 7.0 kcal/mol less stable than the global minimum at the best level of theory. This minimum is quite high in energy because it only presents an intramolecular hydrogen bond set between the NH of the amide group and the nitrogen atom of the *N*-amino moiety. Recent studies indicated that the N–H···N interaction is much less attractive than the N–H···O interaction.^{6e,26}

It should be noted that the fully extended conformation was not characterized as the energy minimum in the PEHS of **2**, while for **3** this is a very stable minimum.⁸ Both, the appearance of additional minima in **2** with respect to **3** and the annihilation of the fully extended conformation as energy minimum indicate that *N*-amination induces drastic conformational changes.

Results in Table 5 show that the relative enthalpies are quite independent of the ab initio method used to optimize the molecular geometries. This is noted in the close similarity between the quantities determined at a given level of theory using HF/6-31G(d) and MP2/6-31G(d) geometries. Thus, the differences were typically around 0.1–0.3 kcal/mol with the exception of the c_2/α_L conformation, for which differences close to 1 kcal/mol were obtained.

On the other hand, a notable dependence of the relative enthalpies on both the basis set and the level of theory was found, even though the t_1/γ_L was the global energy minimum in all cases. Thus, a comparison of the energies provided by the 6-31G(d), 6-311G(d,p), and 6-311++G(d,p) basis sets indicates that the expansion of the basis set usually leads to significant changes. Furthermore, these changes are more important at the MP2 level than at the HF one. The relative enthalpies become smaller as the basis set is enlarged. For instance, the relative enthalpy of t_2/ϵ_D is 4.4 kcal/mol at the MP2/6-31G(d)//MP2/6-31G(d) level. This value decreases to 2.9 kcal/mol at the MP2/6-311++G(d,p)//MP2/6-31G(d). Thus, the reduction due to the extension of the basis set amounts to 1.5 kcal/mol at the MP2 level. However, the change from HF/6-31G(d)//MP2/6-31G(d) to HF/6-311++G(d,p)//MP2/6-31G(d) leads to a reduction in the relative enthalpy of this conformation of only 0.9 kcal/mol. Similar effects are observed in the remaining minima.

The effect of electronic correlation on the relative enthalpies as important as that of basis set. Thus, the change from HF to MP2 level leads, in general, to a stabilization of the conformation. The largest change is obtained for the c_2/α_L . Thus, the relative enthalpies predicted for this conformation at the HF/6-311++G(d,p)//MP2/6-31G(d) and MP2/6-311++G(d,p)//MP2/6-31G(d) levels are 4.0 and 1.9 kcal/mol, respectively. On the other hand, the change from MP2/6-31G(d)//MP2/6-31G(d) to MP4/6-31G(d)//MP2/6-31G(d) introduces very small changes (~0.2 kcal/mol). According to the results displayed in Table 5 and to the preceding discussion, it is expected that calculations at the MP2/6-311++G(d,p)+MP4#//MP2/6-31G(d) level correctly describe the conformational preferences of **2**.

The relative enthalpies of **2** were also determined from DFT calculations. A set of six functionals were chosen for this purpose: B3LYP, SLYP, BVWN, SVWN, B3PW91, and SPW91. Results, which are included in Table 5, indicate a strong basis set effect for all the DFT methods, as noted in the discrepancy of the values determined with the 6-31G(d) and 6-311++G(d,p) basis sets. Indeed, the sensitivity to the basis set extension of the different functionals is similar to that displayed by HF and MP2 methods.

Figure 3 shows the relative enthalpies of the c_2/ϵ_D , t_2/ϵ_D , c_2/α_L , t_2/γ_D , and t_2/α_D conformations plotted against all the DFT

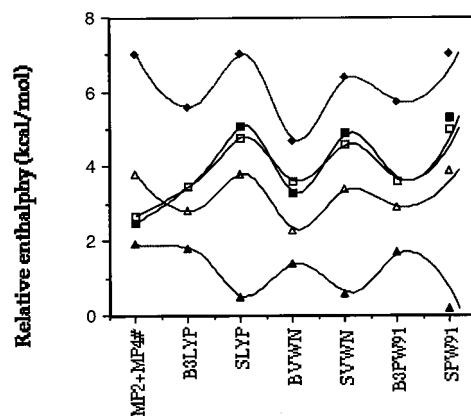


Figure 3. Variation of the relative enthalpies computed with the 6-311++G(d,p) basis set: (▲) c_2/α_L ; (■) c_2/ϵ_D ; (◻) t_2/ϵ_D ; (▽) t_2/γ_D ; (◆) t_2/α_D .

approximations employed here using the 6-311++G(d,p) basis set. Relative enthalpies obtained at the MP2/6-311++G(d,p)+MP4#//MP2/6-31G(d) level have been included for the sake of comparison. All the density functional approximations provide an important discrepancy with respect to the ab initio method. Thus, ab initio calculations predict that the c_2/ϵ_D and t_2/ϵ_D conformations are very close in energy, these two conformations being stabilized with respect to the t_1/γ_D one by more than 1 kcal/mol. All the DFT approximations are able to predict similar enthalpies for the c_2/ϵ_D and t_2/ϵ_D conformations, although their stability is underestimated by about 0.8–2.8 kcal/mol depending on the method. However, the six functionals used in this work predict that these two conformations are less stable than the t_1/γ_D one by about 0.7–1.5 kcal/mol (Figure 3). The strength of the C₇ interaction involved in the latter conformation seems to be overestimated by all the DFT methods. On the other hand, the SLYP, SVWN, and SPW91 approximations overestimate the relative enthalpy of the c_2/α_L conformation by about 1.3–1.7 kcal/mol.

From the study carried out here, it appears that the six density functional methods used are not able to account reasonably for the energetics of **2**. The failures of the density functional methods are probably related with the different type of hydrogen bonds involved in the minimum energy conformations of **2**. Thus, it is well-known that systems with intramolecular hydrogen bonds are particularly difficult for many of the current DFT methods.²⁷

The free energies of solvation (ΔG_{sol}) derived for the five dielectric constants considered ($\epsilon = 2, 4, 8, 33,$ and 78.5) are listed in Table 6. As it was expected, ΔG_{sol} rapidly decreases with the polarity of the surrounding environment. The t_2/α_D conformation, which is less favored in the gas phase, provides the lowest free energy of solvation in the five solvents considered. Moreover, the t_1/γ_L , which is the global minimum in the gas phase, presents the highest free energy of solvation in all cases. The free energy differences in the gas phase (ΔG_{gp}) and in solution (ΔG) are also listed in Table 6.

Results reveal that the solvent plays a crucial role on the stability of the different conformations. The effects induced by the solvent increase with the dielectric constant ϵ . For instance, the c_2/ϵ_D conformation, which in the gas phase is 2.1 kcal/mol less stable than the global minimum, becomes more stable than the t_1/γ_L conformation in environments with $\epsilon \geq 8$. In solvents with $\epsilon \geq 33$, the t_2/γ_D and t_1/γ_L are almost isoenergetic, whereas the former is 3.6 kcal/mol less stable than the latter in the gas phase. However, the largest change is displayed by the t_2/α_D that is the least stable conformation in the gas phase ($\Delta G_{gp} =$

TABLE 6: Free Energy Differences (in kcal/mol) at 298 K in the Gas Phase and Solution between the Six Minimum-Energy Conformations of the Dipeptide Model 2^a

#	t_1/γ_L	c_2/ϵ_D	t_2/ϵ_D	c_2/α_L	t_2/γ_D	t_2/α_D
ΔH_{gp}^b	0.0	2.5	2.7	1.9	3.8	7.0
$-T\Delta S_{gp}^c$	0.0	-0.4	-0.3	-0.7	-0.2	-0.7
ΔG_{gp}^d	0.0	2.1	2.4	1.2	3.6	6.3
$\Delta G_{sol}(\epsilon=2)^e$	-4.8	-5.9	-5.6	-5.2	-6.3	-7.1
$\Delta G(\epsilon=2)^f$	0.0	1.1	1.7	0.8	2.1	4.1
$\Delta G_{sol}(\epsilon=4)^e$	-8.2	-10.1	-9.4	-8.9	-10.6	-12.1
$\Delta G(\epsilon=4)^f$	0.0	0.2	1.2	0.4	1.1	2.4
$\Delta G_{sol}(\epsilon=8)^e$	-10.3	-12.6	-11.7	-11.2	-13.3	-15.2
$\Delta G(\epsilon=8)^f$	0.0	-0.2	1.0	0.3	0.5	1.4
$\Delta G_{sol}(\epsilon=33)^e$	-12.1	-14.8	-13.7	-13.2	-15.7	-18.0
$\Delta G(\epsilon=33)^f$	0.0	-0.6	0.8	0.1	0.0	0.4
$\Delta G_{sol}(\epsilon=78.5)^e$	-12.5	-15.3	-14.1	-13.6	-16.2	-18.6
$\Delta G(\epsilon=78.5)^f$	0.0	-0.7	0.8	0.1	-0.1	0.3

^a Enthalpy and entropic correction differences in the gas phase and free energies of solvation in the different solvents are also displayed (in kcal/mol). Values are relative to the t_1/γ_L conformation. ^b Enthalpies at 298 K in the gas phase calculated at the MP2/6-311++G(d,p)+MP4#//MP2/6-31G(d) level (see Table 4). ^c Entropic corrections at 298 K calculated at the HF/6-31G(d)//HF/6-31G(d) level. ^d Free energy differences at 298 K in the gas phase: $\Delta G_{gp} = \Delta H_{gp} - T\Delta S_{gp}$. ^e Free energies of solvation in solution computed from the PCM model at the HF/6-311++G(d,p)//MP2/6-31G(d) level. ^f Free energy difference at 298 K in solution: $\Delta G = \Delta G_{gp} + \Delta\Delta G_{sol}$.

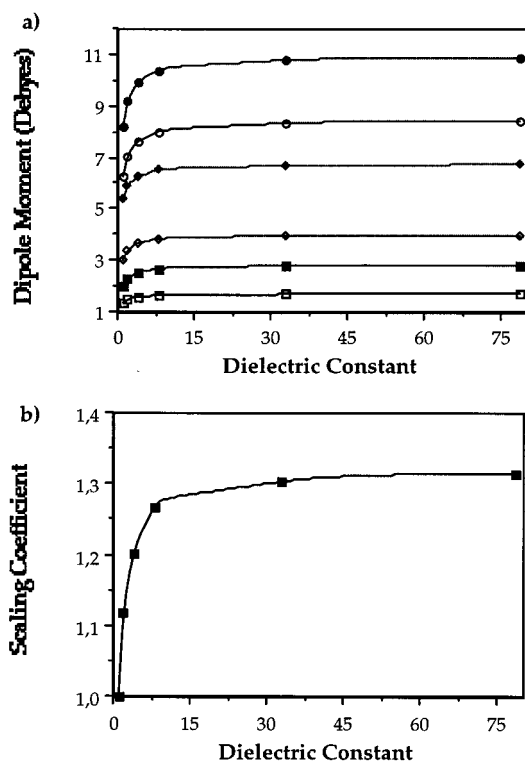


Figure 4. (a) Variation of the dipole moment with the dielectric constant of the solvent for the six minimum-energy conformations of **2**: (\square) t_1/ϵ_L ; (\circ) c_2/ϵ_D ; (\blacksquare) t_2/ϵ_D ; (\diamond) c_2/α_L ; (\blacklozenge) t_2/γ_D ; (\bullet) t_2/α_D . (b) Variation of the scaling coefficient resulting from the comparison between the dipole moments in the gas phase and solution phase (see text) with the dielectric constant of the solvent for **2**.

6.3 kcal/mol). Thus, solvation significantly stabilizes conformation t_2/α_D with respect to t_1/γ_L . The free energy difference decreases to 2.4, 1.4 and 0.3 kcal/mol for $\epsilon = 4, 8,$ and 78.5 , respectively.

Figure 4a shows the variation of the dipole moment with the dielectric constant of the environment for each conformation. As can be seen, for $\epsilon \leq 8$, the solvent-induced polarization effect

TABLE 7: Free Energy Differences (in kcal/mol) at 298 K in the Gas Phase and Aqueous Solution between the More Relevant Minimum-Energy^a Conformations of the Dipeptide Models **4 and **5****

compound	#	ϵ_D	ϵ_D/C_8	γ_D	α_D
4	ΔH_{gp}^b	—	—	0.0 ^c	4.7
	$-T\Delta S_{gp}^d$	—	—	0.0	-0.3
	ΔG_{gp}^e	—	—	0.0	4.4
5	ΔG_{aq}^f	—	—	0.0	3.2
	ΔH_{gp}^b	0.0 ^g	0.8	7.2	—
	$-T\Delta S_{gp}^d$	0.0	-0.1	-0.3	—
	ΔG_{gp}^e	0.0	0.7	6.9	—
	ΔG_{aq}^f	0.0	4.8	6.3	—

^a An empty entry indicates that the conformation was not found as the energy minimum at the HF/6-31G(d) level. Enthalpy and entropic correction differences in the gas phase are also displayed (in kcal/mol). ^b Enthalpies at 298 K in the gas phase calculated at the MP2/6-311G(d,p)//HF/6-31G(d) level. ^c $E = -571.543236$ au. ^d Entropic corrections at 298 K calculated at the HF/6-31G(d)//HF/6-31G(d) level. ^e Free energy differences at 298 K in the gas phase: $\Delta G_{gp} = \Delta H_{gp} - T\Delta S_{gp}$. ^f Free energy difference at 298 K in aqueous solution: $\Delta G = \Delta G_{gp} + \Delta\Delta G_{sol}$. ^g $E = -665.860379$ au.

sharply increases with the dielectric constant, while for $\epsilon > 8$, this variation is smoothed. A quantitative measure of the solvent polarization effect was given by the scaling coefficient (c) provided by the linear regression analysis ($y = cx$) of the solution phase versus the gas-phase dipole moments. The evolution of the scaling coefficient with the dielectric constant of the environment is displayed in Figure 4b. It is worth noting that an organic solvent with $\epsilon = 2$ induces changes in the dipole moments of 12%, which is a small but nonnegligible value. Results predict an increase of 20% and 26% for solvents with $\epsilon = 4$ and 8 , respectively. On the other hand, the changes induced by solvents with $\epsilon = 33$ and 78.5 (30% and 31%, respectively) are the largest ones. However, they only differ in 1% even though the dielectric constant of the latter is more than twice that of the former.

N-Amination of the Proline Dipeptide. To better understand the conformational perturbations induced by *N*-amination in model dipeptides, some calculations were performed on **4** and **5**. Results obtained for the more important minima characterized for such two compounds are summarized in Table 7.

The ϵ_D conformation ($\omega_1 = -178.8^\circ$, $\varphi = 75.1^\circ$, $\psi = -158.0^\circ$, and $\omega_2 = -178.6^\circ$) found by X-ray crystallography for an analogue of **5**,^{7a} i.e., the dipeptide blocked at the *N*-terminus by the ^tBu-CO group rather than by the CH₃-CO group, was used as starting point for complete geometry optimization of **4** and **5** at the HF/6-31G(d) level. The dihedral angles resulting for **5** ($\omega_1 = -176.1^\circ$, $\varphi = 69.8^\circ$, $\psi = -150.0^\circ$, and $\omega_2 = 177.3^\circ$) were in close agreement with those found for the analogue. As can be seen in Figure 5a, this minimum, which was the lowest-energy one for **5**, is mainly stabilized by the interaction between the dipoles rather than by an intramolecular hydrogen bond. In contrast, geometry optimization of **4** led to a γ_D conformation ($\omega_1 = 172.9^\circ$, $\varphi = 86.0^\circ$, $\psi = -75.9^\circ$, and $\omega_2 = 175.6^\circ$), which is stabilized by a C_7 ring. This structure, which is displayed in Figure 5b, also corresponds to the lowest energy conformation of both alanine and glycine dipeptides.⁸

It is worth noting that the substitution of the amide link by the *N*-amino amide one precludes the existence of the C_7 ring. However, a minimum-energy conformation ($\omega_1 = -176.7^\circ$, $\varphi = 55.4^\circ$, $\psi = -128.9^\circ$ and $\omega_2 = 168.1^\circ$) with a C_8 ring was obtained for **5** by changing the orientation of the *N*-amino group (Figure 5c). This conformation, labeled as ϵ_D/C_8 , is 0.7 kcal/

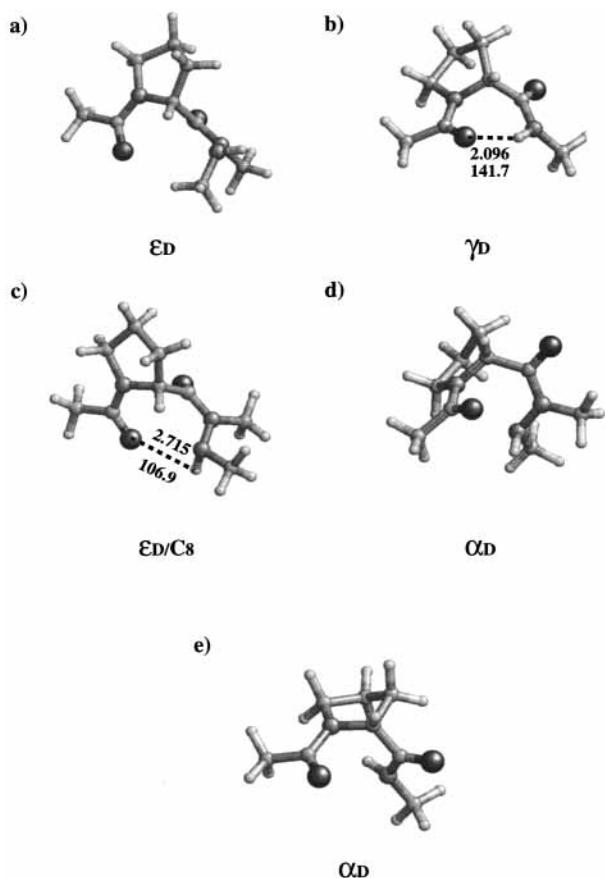


Figure 5. (a) ϵ_D minimum-energy conformation of **5**. (b) γ_D minimum-energy conformation of **4**. (c) ϵ_D minimum-energy conformation of **5** stabilized by a C_8 ring. (d) α_D minimum-energy conformation of **5**. (e) α_D minimum-energy conformation of **4**. Distances and angles in Å and deg, respectively.

less less stable than the global minimum in the gas phase at the MP2/6-311G(d,p)//HF/6-31G(d) level. However, the former conformation becomes 4.8 kcal/mol more stable than the latter one in aqueous solution by computing the free energies of solvation at the HF/6-311++G(d,p) level. It should be mentioned that the stability of the different conformations will be influenced by the chirality of the peptide.

Another interesting point concerns to the helical conformations characterized as minimum for both **4** and **5**. The α_D conformation of **5** ($\omega_1 = 179.0^\circ$, $\varphi = 61.6^\circ$, $\psi = 20.8^\circ$ and $\omega_2 = -169.7^\circ$), which is displayed in Figure 5d, is 6.9 kcal/mol less stable than the global minimum in the gas phase. This free energy difference is 2.5 kcal/mol larger than that obtained for **4** when the γ_D and the α_D (Figure 5e) conformations ($\omega_1 = 171.3^\circ$, $\varphi = 71.2^\circ$, $\psi = 20.2^\circ$, and $\omega_2 = 175.5^\circ$) are compared. On the other hand, for **4**, the stability of α_D conformation increases in aqueous solution by 1.2 kcal/mol. The stabilization of the helical minimum has been also observed in other dipeptides constituted by nonmodified amino acids.²⁴ However, for **5**, the solvent only stabilizes the helical conformation by 0.5 kcal/mol, the α_D minimum being 6.4 kcal/mol less stable than the ϵ_D in aqueous solution.

The above data obtained from ab initio calculations on simple model compounds give an indication on the conformational changes induced by *N*-amination. Results show that introduction of a *N*-amino amide link in a peptide chain significantly perturb the conformation. Therefore, this modification of the amide link can be a useful tool to generate pseudopeptide analogues with specific conformational properties, i.e., peptide design. Studies

in larger compounds to improve our understanding on the perturbations induced by *N*-amination are in progress.

Acknowledgment. This work was supported by the Catalunya Supercomputing Center (CESCA).

References and Notes

- (1) Fasman, G. D. *Prediction of Protein Structure and the Principles of Protein Conformation*; Plenum Press: New York, 1989.
- (2) (a) Alemán, C. *Proteins* **1997**, *29*, 575–582. (b) Seebach, D.; Ciceri, P. E.; Overhand, M.; Jaun, B.; Rigo, D.; Oberer, L.; Hommel, U.; Amstutz, R.; Widmer, H. *Helv. Chim. Acta* **1996**, *79*, 2043. (c) Balaram, P. *Curr. Opin. Struct. Biol.* **1992**, *2*, 845.
- (3) (a) Chorev, M.; Shavitz, R.; Goodman, M.; Minik, S.; Guillemin, R. *Science* **1979**, *204*, 1210. (b) Hintermann, T.; Seebach, D. *Chimia* **1997**, *51*, 244.
- (4) Spatola, A. F. In *Chemistry and Biochemistry of Amino Acids, Peptides and Proteins*; Weinstein, B., Ed.; Marcel Dekker: New York, 1987; Vol. 7, pp 267–357.
- (5) Fletcher, M. D.; Campbell, M. M. *Chem. Rev.* **1998**, *98*, 763.
- (6) (a) Alemán, C.; Pérez, J. J. *J. Mol. Struct. (THEOCHEM)* **1993**, *285*, 221. (b) Sandrone, G.; Dixon, D. A.; Hay, B. P. *J. Phys. Chem. A* **1999**, *103*, 3554. (c) Alemán, C.; Puiggali, J. *J. Org. Chem.* **1995**, *60*, 910. (d) Alemán, C. *J. Biomol. Struct. Dyn.* **1996**, *14*, 193. (e) Alemán, C. *J. Phys. Chem.* **2001**, *105*, 860.
- (7) (a) Dupont, V.; Lecoq, A.; Mageot, J.-P.; Aubry, A.; Boussard, G.; Marraud, M. *J. Am. Chem. Soc.* **1993**, *115*, 8898. (b) Marraud, M.; Dupont, V.; Grand, V.; Zerkout, S.; Lecoq, A.; Boussard, G.; Vidal, J.; Collet, A.; Aubry, A. *Biopolymers* **1993**, *33*, 1135. (c) Vidal, J.; Drouin, J.; Collet, A. *J. Chem. Soc. Chem. Commun.* **1991**, 435. (d) Vidal, J.; Drouin, J.; Collet, A. *Tetrahedron* **1987**, *43*, 891.
- (8) (a) Böhm, H.-J.; Brode, S. *J. Am. Chem. Soc.* **1991**, *113*, 7129. (b) Head-Gordon, T.; Head-Gordon, M.; Frisch, M. J.; Brooks, C. L., III.; Pople, J. A. *J. Am. Chem. Soc.* **1991**, *113*, 5989. (c) Gould, R.; Kollman, P. A. *J. Phys. Chem.* **1992**, *96*, 9255. (d) Jensen, J. H.; Gordon, M. S. *J. Am. Chem. Soc.* **1991**, *113*, 7917. (e) Hu, C. H.; Sehn, M.; Schaefer, H. F., III. *J. Am. Chem. Soc.* **1993**, *115*, 2923. (f) Cornell, W. D.; Gould, I. R.; Kollman, P. A. *J. Mol. Struct.* **1997**, *392*, 101. (g) Sirois, S.; Prynov, E. I.; Nguyen, D. T.; Salahub, D. R. *J. Chem. Phys.* **1997**, *107*, 6770.
- (9) (a) Boussard, G.; Marraud, M.; Aubry, A. *Biopolymers* **1979**, *18*, 1297. (b) Boussard, G.; Marraud, M. *J. Am. Chem. Soc.* **1985**, *107*, 1825. (c) Liang, G. B.; Rito, C. I.; Gellman, S. H. *Biopolymers* **1992**, *32*, 293.
- (10) Frisch, M. J.; Trucks, G. W.; Schlegel, H. B.; Scuseria, G. E.; Robb, M. A.; Cheeseman, J. R.; Zakrzewski, V. G.; Montgomery, J. A., Jr.; Stratmann, R. E.; Burant, J. C.; Dapprich, S.; Millam, J. M.; Daniels, A. D.; Kudin, K. N.; Strain, M. C.; Farkas, O.; Tomasi, J.; Barone, V.; Cossi, M.; Cammi, R.; Mennucci, B.; Pomelli, C.; Adamo, C.; Clifford, S.; Ochterski, J.; Petersson, G. A.; Ayala, P. Y.; Cui, Q.; Morokuma, K.; Malick, D. K.; Rabuck, A. D.; Raghavachari, K.; Foresman, J. B.; Cioslowski, J.; Ortiz, J. V.; Stefanov, B. B.; Liu, G.; Liashenko, A.; Piskorz, P.; Komaromi, I.; Gomperts, R.; Martin, R. L.; Fox, D. J.; Keith, T.; Al-Laham, M. A.; Peng, C. Y.; Nanayakkara, A.; Gonzalez, C.; Challacombe, M.; Gill, P. M. W.; Johnson, B. G.; Chen, W.; Wong, M. W.; Andres, J. L.; Head-Gordon, M.; Replogle, E. S.; Pople, J. A. *Gaussian 98*; Gaussian, Inc.: Pittsburgh, PA, 1998.
- (11) Hariharan, P. C.; Pople, J. A. *Chem. Phys. Letter* **1972**, *16*, 217.
- (12) Møller, C.; Plesset, M. S. *Phys. Rev.* **1934**, *46*, 618.
- (13) Slater, J. C. *The Self-Consistent Field for Molecules and Solids; Quantum Theory of Molecules and Solids*; McGraw-Hill: New York, 1974; Vol. 4.
- (14) Vosko, S. H.; Wilk, L.; Nusair, M. *Can. J. Phys.* **1980**, *58*, 1200.
- (15) Becke, A. D. *Phys. Rev. A* **1988**, *38*, 3098.
- (16) Lee, C.; Yang, W.; Parr, R. G. *Phys. Rev. B* **1993**, *37*, 785.
- (17) (a) Becke, A. D. *J. Chem. Phys.* **1993**, *98*, 1372. (b) Stephens, P. J.; Devlin, F. J.; Chabalowski, C. F.; Frisch, M. J. *J. Phys. Chem.* **1994**, *98*, 1623.
- (18) Perdew, J. P. In *Electronic Structure of Solids*; Ziesche, P., Eschrig, H., Eds.; Academic Verlag: Berlin, Germany, 1991.
- (19) Miertus, S.; Scrocco, E.; Tomasi, J. *J. Chem. Phys.* **1981**, *55*, 117.
- (20) (a) Drakenberg, J. T.; Forsen, S. *J. Chem. Soc., Chem. Commun.* **1971**, 3683. (b) Cabani, S.; Gianni, P.; Mollica, U.; Lepori, L. *J. Solut. Chem.* **1981**, *10*, 563. (c) Jorgensen, W. L.; Gao, J. *J. Am. Chem. Soc.* **1988**, *110*, 4212. (d) Duffy, E. M.; Severance, D. L.; Jorgensen, W. L. *J. Am. Chem. Soc.* **1992**, *114*, 7535. (e) Harrison, R. K.; Stein, R. L. *J. Am. Chem. Soc.* **1992**, *114*, 3464. (f) Luque, F. J.; Orozco, M. *J. Org. Chem.* **1993**, *58*, 6397. (g) Wiberg, K. B.; Rablen, P. R. *J. Am. Chem. Soc.* **1995**, *117*, 2201. (h) Knight, E. T.; Allen, L. C. *J. Am. Chem. Soc.* **1995**, *117*,

4401. (i) Pusheng, L.; Chen, X. G.; Shulin, E.; Asher, S. A. *J. Am. Chem. Soc.* **1997**, *119*, 1116. (j) Holtz, J. S. W.; Pusheng, L.; Asher, S. A. *J. Am. Chem. Soc.* **1999**, *121*, 3762.

(21) Drakenberg, J. T.; Forsen, S. *J. Chem. Soc., Chem. Commun.* **1971**, 3683.

(22) Cabani, S.; Gianni, P.; Móllica, U.; Lepori, L. *J. Solut. Chem.* **1981**, *10*, 563.

(23) Perczel, A.; Ángyán, J. G.; Kajtár, M.; Viviani, W.; Rivail, J.-L.; Marcoccia, J. F.; Csizmadia, I. G. *J. Am. Chem. Soc.* **1991**, *113*, 6256.

(24) (a) Alemán, C.; Puiggali, J. *J. Phys. Chem.* **1997**, *101*, 3441. (b) Alemán, C. *J. Phys. Chem. A* **2000**, *104*, 7612.

(25) Aubry, A.; Del Duca, V.; Pedone, C.; Zerkout, S.; Marroud, M. *Acta Crystallogr.* **1999**, *C55*, 439.

(26) (a) Alemán, C. *J. Phys. Chem. B* **2001**, *105*, 860. (b) Alemán, C.; León, S. *THEOCHEM* **2000**, *505*, 211.

(27) (a) Del Bene, J. E.; Person, W. B.; Szczepaniak, K. *J. Phys. Chem.* **1995**, *99*, 10705. (b) Sirois, S.; Proynov, E. I.; Nguyen, D. T.; Salahub, D. R. *J. Chem. Phys.* **1997**, *107*, 6770.